10.1109/ULTSYM.2013.0491

Modeling of Inter-digitated Transducer for High-order Contour Mode Resonators

Renyuan Wang and Sunil A. Bhave
ECE Department
Cornell University
Ithaca, USA

Kushal Bhattacharjee
RF Micro Devices, Inc.
Greensboro, USA

***Abstract*—$LiNbO_3$ contour-mode resonators (CMR) have the potential to fulfill the requirement of multi-frequency wide-band-pass filters. For CMRs, the position of the inter-digitated transducer (IDT) fingers can significantly affect their performance [1], as the reflection of acoustic waves at the sharply defined mechanical boundaries cause strong interferences of these waves. In this paper, we present a model that analytically & intuitively explains the behavior of CMRs with IDT at the mechanical anti-nodes (AN) of the targeted mechanical mode vs. with IDT at the nodes (N). The model is then verified with experimental results.**

Keywords—Lithium Niobate, contour mode resonator, delta function model, inter-digitated transducer

I. Introduction

The three necessary conditions to speed-up adoption of contour-mode resonators (CMR) for multi-frequency band-select filters in wireless communications are: low motional impedance, high electromechanical coupling factor (k_t^2) and spur-free wide-band response. Thin-film Lithium Niobate (LN) is a superior technology platform that meets the wireless industry requirements for the first two. However, as k_t^2 increases, both Cornell and CMU groups [1,2] have noticed increased "spur"-ious activity across a wide-span of frequencies right adjacent to the desired resonance. In [1], we showed preliminary results of an "Anti-Node" (AN) IDT transducer, where the IDT fingers are placed at the anti-nodes of the targeted mechanical mode, as opposed to placement at the nodal points, a configuration commonly used for Aluminum Ntride (AlN) CMRs. Fig. 1 shows cross-sections of resonators with the two different IDT configurations. For a thin plate with a total width of $N\times\lambda_0/2$, the N^{th} order mode corresponds to a wavelength of λ_0. Both IDTs have $\lambda_0/4$ finger pairs with a period of $\lambda_0/2$. The AN IDT fingers are placed at the mechanical anti-nodes of the N^{th} order mode with two additional $\lambda_0/8$ fingers right at the edges of the resonator, while the N IDT fingers are placed at the mechanical nodes. Compared to the N IDT, the AN IDT shows strong suppression of spurious modes and high k_t^2 [1]. This originates from the fact that the strong reflection of acoustic wave from the boundaries of the free-standing resonator body causes multiple reflections of the acoustic waves which interfere with themselves forming an equivalent mechanical Fabry-Perot cavity. Depending on the relative positions of the electrodes and the mechanical boundaries, the interferences can be constructive or destructive, resulting in reinforcement or suppression of mechanical modes. In this paper, we present a mathematical treatment and analytical model, that explains the behavior of the AN vs. N responses. These modes are compared closely to experimental results for validation. The model will help identify design parameters that should be optimized in design and layout to further improve the performance of LN CMRs.

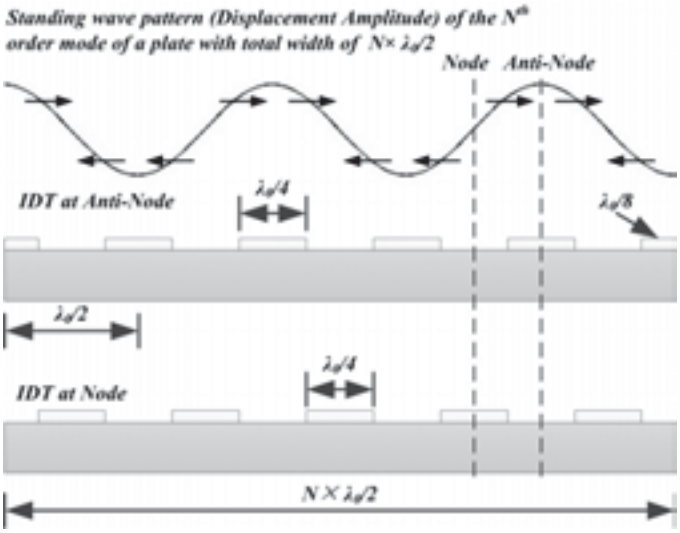

Fig. 1: Comparison of IDT configurations: IDT placed at anti-nodes (top) and nodes (bottom) of the targeted mechanical mode.

II. Derivation

Following the traditional delta function mode for surface acoustic wave devices [3,4], we start our derivation by treating each electrode finger as point source emitting acoustic waves. The collective frequency response of all fingers is achieved by summing the contributions from each finger at a reference point. However, for IDT on contour mode resonators, the key is to include the effect of the scattering of acoustic waves at the device boundaries. For example, Fig. 2 shows the configurations of both AN and N IDT devices with total width of $N\times\lambda_0/2$, where N is even. Therefore, the nodal IDT has N finger electrodes and the AN IDT has $N+1$ fingers, while the potentials on the fingers are anti-symmetric for the nodal type

This work is supported by the DARPA ART program.

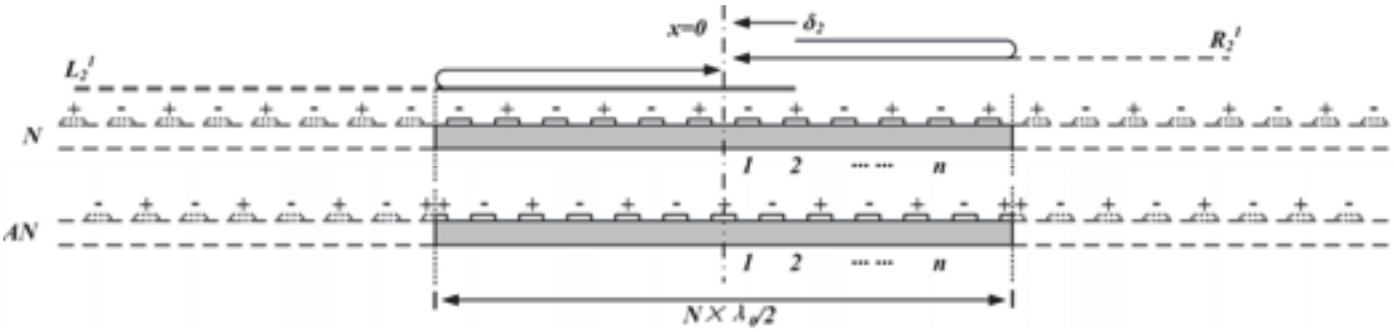

Fig. 2: Schematic of nodal IDT and anti-nodal IDT with a total period of N, the black solid arrow lines mark the path of reflected acoustic waves and the dash lines mark the equivalent path from the mirror images.

and symmetric for AN type with respect to $x=0$. We first consider the nodal IDT. At $x=0$, the motion caused by the acoustic wave emitted by the n^{th} finger to the right of $x=0$ can be written as

$$\delta_n = (-1)^n A_{Node} e^{-j\beta[-(\frac{n\lambda_0}{2}-\frac{\lambda_0}{4})]} \tag{1}$$

where $\beta = 2\pi/\lambda_0 = 2\pi f/V_0$, and V_0 is the acoustic wave velocity for λ_0. A_{Node} is the frequency dependent element factor of the IDT. On the other hand, the motion caused by the reflected wave emitted by the n^{th} finger can be viewed as motion caused by the wave emitted by its mirror images as shown in Fig. 2. They can be expressed as

$$R_n^m = \alpha^m (-1)^n A_{Node} e^{j\beta\left[mN\frac{\lambda_0}{2}+(-1)^m(\frac{n\lambda_0}{2}-\frac{\lambda_0}{4})\right]} \tag{2}$$

$$L_n^m = \alpha^m (-1)^n A_{Node} e^{-j\beta\left[mN\frac{\lambda_0}{2}+(-1)^{m-1}(\frac{n\lambda_0}{2}-\frac{\lambda_0}{4})\right]} \tag{3}$$

where R_n^m is the motion caused by the wave reflected from the right boundary. m indicates the wave has been reflected by m times from either boundaries, and n indicates the wave is emitted by the n^{th} finger to the right of $x=0$. Similarly, L_n^m is the motion caused by wave reflected by the left boundary. α is the loss factor associated with the scattering loss at the mechanical boundaries, where $\alpha=1$ means total reflection. The total frequency response of the nodal IDT can be written as

$$H_{Node}(f) = h_{Node}(f) + h^S_{Node}(f) \tag{4}$$

where $h_{Node}(f)$ is the frequency response without considering the scattering form the boundaries. As the electrical potential on each finger is anti-symmetric about $x=0$, it can be expressed as

$$h_{Node}(f) = A_{Node}\sum_1^{N/2}(-1)^n\left(e^{j\pi(n-\frac{1}{2})\frac{f}{f_0}} - e^{-j\pi(n-\frac{1}{2})\frac{f}{f_0}}\right) \tag{5}$$

and $h^S_{Node}(f)$ is the summation of the R_n^m and L_n^m terms from all the fingers for all m, which can be written as

$$h^S_{Node}(f) = h_{Node}(f) * \left\{\mathrm{Re}\left[\frac{1-\alpha e^{j\pi N\frac{f}{f_0}}}{1-\alpha^2 e^{j2\pi N\frac{f}{f_0}}}\right]-1\right\} \tag{6}$$

which finally yields the expression for $H_{Node}(f)$ as

$$H_{Node}(f) = A_{Node}h_{Node}\,\mathrm{Re}\left[\frac{1-\alpha e^{j\pi N\frac{f}{f_0}}}{1-\alpha^2 e^{j2\pi N\frac{f}{f_0}}}\right] \tag{7}$$

Here, we neglect the dispersion of acoustic wave velocity, as the frequencies of the parasitic modes are generally close to the targeted mode. Similarly, the frequency response of the AN IDT can be written as,

$$H_{ANode}(f) = A_{ANode}h_{ANode}\,\mathrm{Re}\left[\frac{1+\alpha e^{j\pi N\frac{f}{f_0}}}{1-\alpha^2 e^{j2\pi N\frac{f}{f_0}}}\right] \tag{8}$$

where h_{ANode} is the IDT frequency response without considering the boundary reflections, and the term in the bracket reflects the effect of boundary scattering.

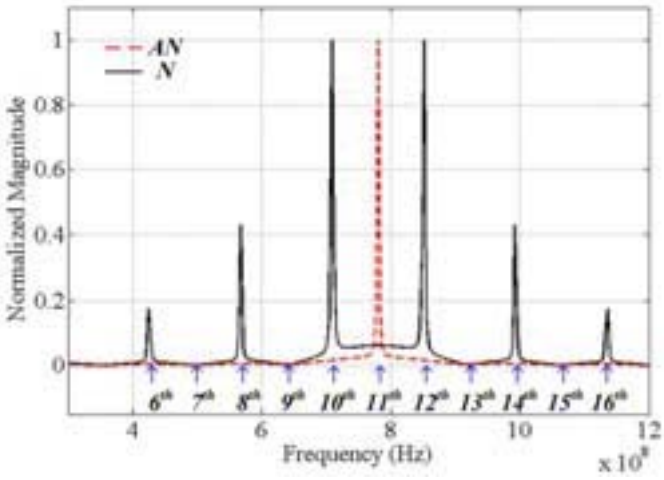

Fig. 3: Normalized magnitude of $H_{ANode}(f)$ and $H_{Node}(f)$, where blue arrows mark the frequencies of different mechanical modes.

TABLE I. DESIGN PARAMETERS USED FOR CALCUALTION OF THE FREQUENCY RESPONSE IN FIG. 3

	Total Width	*Number of Fingers*	f_0	α	A
AN IDT	11* $\lambda_0/2$	12	780MHz	0.95	1
N IDT	11* $\lambda_0/2$	11	780MHz	0.95	1

The presented derivation is based on devices with an even number of periods, while the model for devices with an odd number of periods can be derived using similar procedures, which yields similar forms. Fig. 3 plots the normalized magnitude of $H_{ANode}(f)$ and $H_{Node}(f)$ using the parameters shown in Table 1, where N is odd.

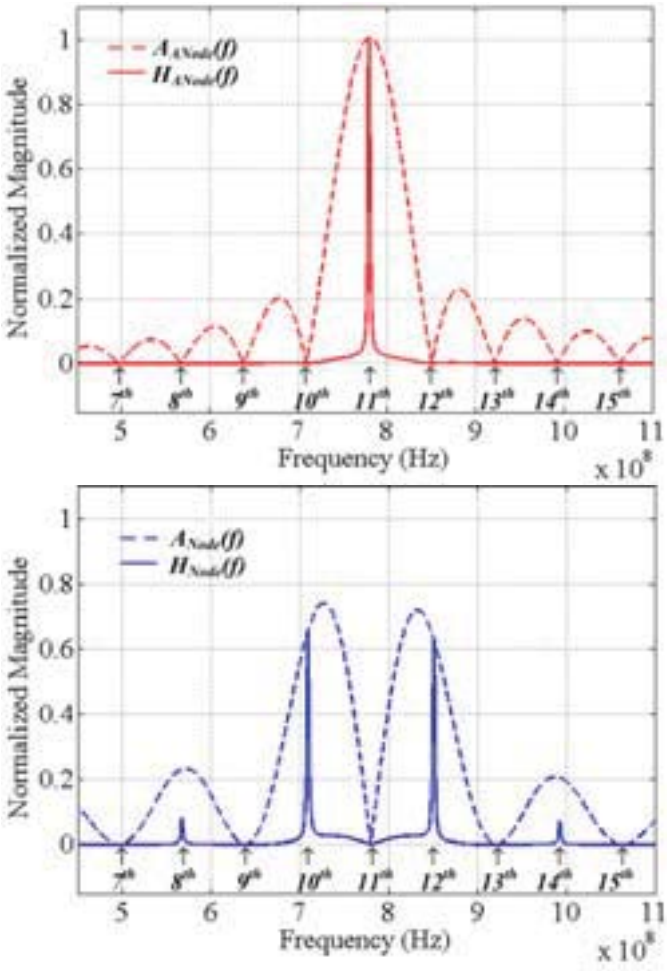

Fig. 4: Frequency dependent $A_{Node}(f)$ and $A_{Anode}(f)$, and the final frequency response $H_{ANode}(f)$ and $H_{Node}(f)$.

The blue arrows mark the frequencies of different mechanical modes. The peculiar feature of the N IDT is that it strongly suppresses the odd order modes as they coincide with the zeros of the frequency response, while exciting the even order modes, even though it has 11 fingers and the total device width is 11× $\lambda_0/2$. On the other hand, the AN IDT strongly suppresses all other modes except the 11th order mode (780MHz). As a result, the AN IDT is preferred where clean wide band spectrum is required. It is worth noting that the AN IDT also couples to the odd order harmonics of the 11th order mode. However, in reality, these modes are at frequencies over a few GHz, where the mechanical loss renders them un-measureable.

Finally, we assumed A is 1 for all frequencies in Fig. 3. However, as previously mentioned, it also depends on the overlap integral of the charge distribution on the fingers and the mechanical mode profile. For simplicity, the overlap integral is evaluated by treating the mechanical motion as 1D travelling wave and the charge distribution as square wave. Fig. 4 shows the magnitude of $A_{Node}(f)$ and $A_{Anode}(f)$ normalized to the peak value of $A_{Anode}(f)$, and the final $H_{ANode}(f)$ and $H_{Node}(f)$ including the effect of the frequency dependent element factor. For the AN IDT, the frequency dependent element factor actually reinforces the suppression of parasitic modes.

III. EXPERIMENTAL RESULTS

First, Fig. 5 shows the measured admittance of two resonators designed for operating at ~800MHz from [1]. It shows very good agreement between measurement and model. Both devices have an IDT period of 3.8um, a total width of 11*3.8um, and a metallization ratio of 0.5, the only difference is the electrode configuration (AN vs. N). As predicted by the model, the AN IDT excites the 11th order S_0 mode (787.9MHz), while all other modes are strongly suppressed by more than 30dB. The minor spur very close to parallel resonance of the 11th order mode is the same order A_0 with very low coupling factor. In contrast, the N IDT spectrum shows several spurious peaks, where it couples strongly to the even order modes adjacent to the strongly suppressed 11th order mode. The average spacing of the even order modes is ~148MHz, which agrees with the mode spacing for the CMR. The AN IDT has higher coupling factor as expected from the larger magnitude of frequency response at resonance.

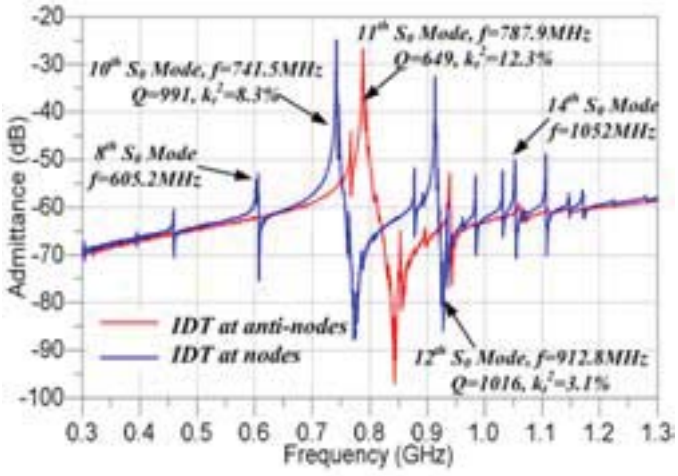

Fig. 5: Measured admittance of two resonators with the exactly same design parameters, except they have different electrode configurations (AN vs. N) [1].

To further verify the model, resonators with different electrode configurations were fabricated following the fabrication process in [1]. Fig. 6 shows two more resonators with AN and N type IDTs, both with total widths of 21*3.8um.

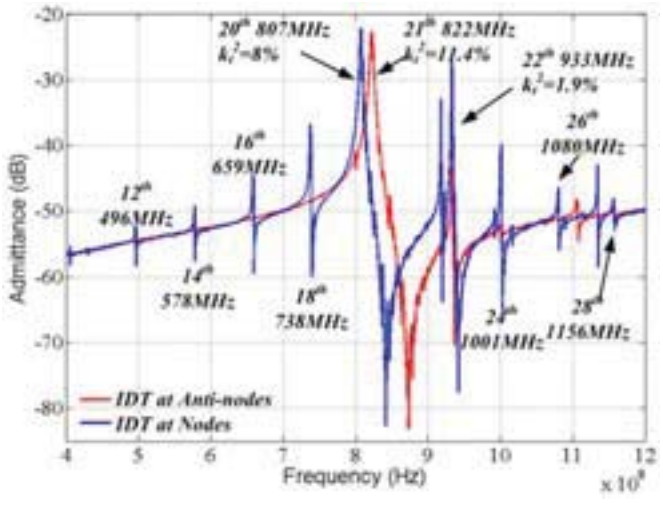

Fig. 6: Measured admittance of two resonators with different electrode configurations, where the two resonators both have 21 periods.

The N IDT only couples to the even order modes, while the AN IDT shows a clean spectrum with only one strong resonance. The average frequency spacing of the N IDT is 82.5MHz, which is twice the frequency spacing for the mechanical modes of the resonators. It is worth noting that the 21st order mode of the AN type is not centered between the two major peaks of the N IDT device. This is because mass loading effects are stronger for the AN type as the electrodes are at positions with maximum displacement. Therefore the 21st order mode is shifted to a lower frequency.

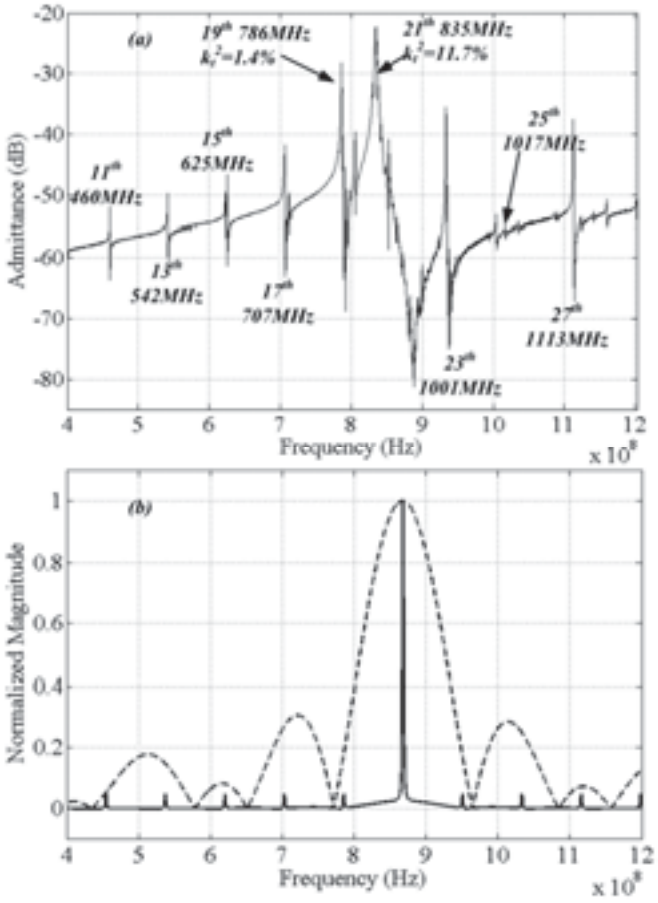

Fig. 7: (a)Measured admittance of a AN IDT device without the edge $\lambda_0/8$ fingers; (b) Frequency response of the aforementioned IDT from the analytic model.

Finally, Fig. 7a shows the measured admittance of a special device with the same design as the AN device shown in Fig. 6, except without the two $\lambda_0/8$ fingers on the edges. Fig. 7b shows the frequency response calculated from the analytic model, showing good qualitative agreement with the measurement. Interestingly, by missing only two edge fingers, the IDT can no longer provide strong suppression of parasitic modes, as the contribution from the edge fingers to the destructive interference of the acoustic waves is missing. This also highlights difficulties in the fabrication process. For typical GHz resonators, λ_0 is in the range of a few microns, which means mis-alignment on the order of 0.1um can significantly affect the frequency response.

In conclusion, we proposed a mathematical model for analyzing IDTs of high order CMRs. We discuss the frequency response of IDT@AN and IDT@N and their impact on resonator spurious response. The model has excellent agreement with experimental results. Our model provides a non-FEA toolset that can be programmed into ADS for filter design and is applicable to any piezo CMR technology including PZT, AlN and AlScN.

ACKNOWLEDGMENT

The authors wish to thank the DARPA ART program, whose generous grant has made this research possible. We would also like to thank Dr. Seungbae Lee, Professor Sheng-Shian Li, Dr. Warren Welch, and Dr. Jason Reed for initial work on LN resonator and process development in RFMD. This work was performed in part at the Cornell NanoScale Facility, a member of the National Nanotechnology Infrastructure Network, which is supported by the National Science Foundation (Grant ECCS-0335765).

REFERENCES

[1] R. Wang, S. A. Bhave, and K. Bhattacharjee, "High $k_t^2 \times Q$, multi-frequency Lithium Niobate Resonators", *Micro Electro Mechanical Systems (MEMS), 2013 IEEE 26th International Conference on,* pp.165, 2013.

[2] S. Gong, G. Piazza, "Design and analysis of Lithium-Niobate-Base high electromechanical coupling RF-MEMS resonators for wideband filters", *Microwave Theory and Tehchniques, IEEE Tran.,*vol. 61, no.1, pp403, 2013.

[3] M. Kadota, et al., "Very small IF resonator filters using reflection of shear horizontal wave at free edges of substrate", *Tran. UFFC*, pp. 1269-1279, 49 (2002).

[4] R. H. Tancrell, and M. G. Holland, "Acoutic surface wave filters", *Proceedings of the IEEE*, pp. 393-409, 59 (1971).